

Photodynamic inactivation of methicillin-resistant *Staphylococcus aureus* and *Escherichia coli*: A metalloporphyrin comparison

Troy A. Skwor^{a,b,*}, Stephanie Klemm^a, Hanyu Zhang^c, Brianna Schardt^a,
Stephanie Blaszczyk^a, Matthew A. Bork^a

^a Rockford University, Department of Chemical and Biological Sciences, 5050 E. State St., Rockford, IL 61108, USA

^b University of Illinois – Chicago at Rockford, College of Medicine, 1601 Parkview Ave., Rockford, IL 61107, USA

^c Purdue University, School of mechanical engineering, 585 Purdue Mall, West Lafayette, IN 47907, USA

ARTICLE INFO

Article history:

Received 2 August 2016

Received in revised form 10 October 2016

Accepted 14 October 2016

Available online 15 October 2016

Keywords:

TMPyP

MRSA

E. coli

PDI

Singlet oxygen

Metalloporphyrin

ABSTRACT

Increasing rates of antibiotic resistance coupled with the lack of novel antibiotics threatens proper clinical treatment and jeopardizes their use in prevention. A photodynamic approach appears to be an innovative treatment option, even for multi-drug resistant strains of bacteria. Three components are utilized in photodynamic inactivation: a photosensitizer, light source, and oxygen. Variations in photosensitizers strongly influence microbial binding and bactericidal activity. In this study, four different cationic metalloporphyrins (Cu^{2+} , Fe^{2+} , Pd^{2+} , Zn^{2+}) were compared to the free-base ligand 5,10,15,20-tetrakis(*N*-methylpyridinium-4-yl)porphyrin regarding their electronic properties and generation of reactive oxygen species upon subsequent 405 nm violet-blue irradiation. *Staphylococcus aureus* and *Escherichia coli* were used as representatives of Gram-positive and -negative, respectively, to assess bactericidal effects by the photodynamic process. Bacterial cultures were pre-incubated with porphyrins and exposed to varying doses of 405 nm irradiation (0–30 J/cm²). Metalloporphyrins containing Cu^{2+} and Fe^{2+} demonstrated minimal effects on viability. Pronounced bactericidal activity was evident with free-base ligand, Zn^{2+} , and Pd^{2+} ; though significantly stronger effects were apparent with Pd^{2+} . Photodynamic killing was directly proportional to reactive oxygen species production post-illumination. These data provide new insight into the influence of metal chelation on photosensitizer activity on bactericidal singlet oxygen production. The strong anti-microbial photodynamic action through the use of a portable light-emitting diode over short time intervals (seconds) provides support for its potential use in self-treatment.

© 2016 The Authors. Published by Elsevier B.V. This is an open access article under the CC BY-NC-ND license (<http://creativecommons.org/licenses/by-nc-nd/4.0/>).

1. Introduction

Annually, approximately two million people in the United States acquire bacterial infections that are resistant to antibiotics with 23,000 ensuing deaths [1]. The economic burden of this epidemic claims \$20 billion annually in healthcare-associated costs with an additional \$35 billion lost due to decreased productivity [2]. Over the last half century, clinical and animal isolates continue to display an alarming upward trend of anti-microbial resistance [3]. This surge in resistant phenotypes can be attributable to the inappropriate use, close proximity of human and animals [4], and improper disposal of antibacterial drugs [5].

Abbreviations: MRSA, methicillin-resistant *Staphylococcus aureus*; PDI, photodynamic inactivation; PDT, photodynamic therapy; T4, 5,10,15,20-tetrakis(*N*-methylpyridinium-4-yl)porphyrin; ANOVA, analysis of variance.

* Corresponding author at: Rockford University, Department of Chemical and Biological Sciences, 5050 E. State St., Rockford, IL 61108, USA.

E-mail addresses: tskwor@rockford.edu (T.A. Skwor), stephmarie2626@gmail.com (S. Klemm), zhang220@purdue.edu (H. Zhang), bjschardt@me.com (B. Schardt), stephblaszczyk8@gmail.com (S. Blaszczyk), mbork@rockford.edu (M.A. Bork).

Escherichia coli are Gram-negative, facultative anaerobic bacteria which inhabit the gastrointestinal tract of warm-blooded mammals. However, *E. coli* is also a well-known etiological agent for gastrointestinal and urinary tract infections in both nosocomial and community-acquired infections. The emergence of extended-spectrum β -lactamases (ESBL) amongst *Enterobacteriaceae* and the first human documented case of resistance to colistin, a last-line treatment for ESBL isolates [6], re-emphasizes the dwindling clinical efficacy of antibiotics.

Beyond Gram-negative bacteria, a similar story prevails amongst Gram-positive bacteria where antibiotic resistant strains of *Staphylococcus aureus* continue to emerge globally [7]. This pathogenic bacterium is responsible for an array of infections including skin, soft tissue, lower respiratory tract, and septicemia. Community and healthcare-acquired methicillin-resistant strains of *Staphylococcus aureus* (MRSA) has dramatically increased [8,9] and claimed over 11,000 lives in the United States in 2011 [1]. Vancomycin, a standard treatment for MRSA, shares an analogous fate where the first resistant case presented in 2002 [10], with succeeding clinical cases of vancomycin-intermediate *Staphylococcus aureus* rising to 7.9% by 2014 [11].

Since the rate of antibiotic-resistance acquisition is inversely proportional to deficiency in antibiotic discovery, an alternative treatment is imperative. Photodynamic treatment is one example that has shown promise combating numerous bacterial, viral, fungal and protozoan infections [12–16]. Benefits over antibiotics in clinical settings include localized wound application and minimal side effects, resistance, and toxicity [17]. In contrast to antibiotics, sub-inhibitory doses of photodynamic inactivation (PDI) have failed to induce genomic mutations and elevate antibiotic or photodynamic resistance [18,19]. This therapeutic approach utilizes visible light, a photosensitizer, and molecular oxygen to create reactive oxygen species (ROS) resulting in bacterial cell death [20]. An array of chemicals including porphyrins, phthalocyanines, phenothiazines, dyes, chlorines, and acridines have been used as photosensitizers. Specifically, cationic porphyrins like 5,10,15,20-tetrakis(*N*-methylpyridinium-4-yl)porphyrin have shown strong anti-microbial properties to both Gram-positive and -negative bacteria [21,22]; however, modifications of porphyrins could be implemented to enhance inactivation.

The purpose of this study was to investigate antimicrobial effects of PDI using different metalloporphyrins as photosensitizing agents. Cationic porphyrins, as mentioned above, interact with a diverse array of bacterial species. However, subtle changes in the electronic properties of photosensitizers can enhance intersystem crossing thus heightening ROS production and photodynamic damage [23]. Electronic properties can be modified by altering the porphyrin core through metal chelation. This study investigated singlet oxygen production and bactericidal effects against model bacterial pathogens *E. coli* and MRSA using Cu^{2+} , Fe^{2+} , Pd^{2+} , and Zn^{2+} inserted into the tetra-cationic porphyrin. A portable hand-held device with 405 nm light-emitting diodes (LED) was utilized for photosensitizer excitation, thus highlighting its potential as a self-applied treatment for wound infections.

2. Materials and Methods

2.1. Bacterial Culturing and Quantification

E. coli ATCC 11775 and MRSA ATCC 43300 strains were obtained from frozen stocks and cultures grown at 37 °C in tryptic soy broth (TSB). Overnight cultures were centrifuged at 8161 x g for 5 min (Eppendorf 5415C, Germany). Cell pellets were washed with 0.85% sterile NaCl (saline) at pH 7.4 and resuspended in 1 ml sterile saline. *E. coli* and MRSA were further diluted in saline to a 0.5 McFarland standard.

2.2. Development of Metalloporphyrins

Metalloporphyrins were synthesized following previously published procedures [24–26]. Briefly, an ion exchange of 5,10,15,20-tetrakis(*N*-methylpyridinium-4-yl)porphyrin tetra(4-toluenesulfonate) yielded the $[\text{H}_2(\text{T4})](\text{PF}_6)_4$ salt, which was then dissolved in acetonitrile and precipitated with acetone containing tetrabutylammonium nitrate (TBAN). The resulting $[\text{H}_2(\text{T4})](\text{NO}_3)_4$ was solubilized in distilled water and refluxed overnight with a ten-fold molar excess of a metallic salt: zinc(II) acetate, copper(II) acetate, iron(II) chloride, or $\text{Pd}(\text{DMSO})_2(\text{H}_2\text{O})_2$ to create various metalloporphyrins. $\text{Pd}(\text{DMSO})_2(\text{H}_2\text{O})_2$ was synthesized as previously described [27]. Molecular absorption spectroscopy via GENSYSTEM™ 10S UV-Vis Spectrophotometer (Thermo Scientific, MA, USA) was utilized to ensure metal ion insertion. The metalloporphyrin solutions were filtered and isolated by precipitation via addition of KPF_6 in acetonitrile. Ion exchange with TBAN yielded water soluble metalloporphyrins as nitrate salts which were further characterized via absorption spectroscopy to determine concentration and absorption spectra, thus highlighting Soret peaks.

2.3. Determination of Bacterial Binding to Metalloporphyrin

Bacterial suspensions of MRSA and *E. coli* were diluted to a McFarland 0.5 standard with 0.85% sterile saline and incubated with

10 μM of Pd(T4) for 5 min. After incubation, the samples were centrifuged at 8161 x g, washed, and subsequently resuspended in 0.85% sterile saline. Absorption spectra of the samples were obtained and normalized. Considering the additive nature of absorbance, quantification of the Pd(T4) interaction with bacteria was estimated from residual Soret peak (at 418 nm) superimposed on the bacterial absorbance.

2.4. Photodynamic Inactivation and Determination of Cell Viability

Preliminary effects of various porphyrins ($\text{Cu}(\text{T4})$, $\text{Fe}(\text{T4})$, $\text{H}_2(\text{T4})$, $\text{Pd}(\text{T4})$, and $\text{Zn}(\text{T4})$) against bacterial growth were investigated in 96-well plates. Briefly, 100 μl of MRSA with or without different concentrations of porphyrins were inoculated into wells for 5 min in the dark. Wells were exposed to 405 nm LED (WARP, Quantum Devices, Inc., OH, USA) at 60 mW/cm^2 for 44 s producing 2.5 J/cm^2 and placed on an orbital shaker (MidSci, MO, USA) for 7 h at 200 rpm. Growth was defined by turbidity measurements at 570 nm using an ELx800 Absorbance Microplate Reader (Biotek, VT, USA) post-7 h. After the most effective photosensitizers were identified, bactericidal activity was tested on 2 ml of bacterial culture in 10×60 mm plates (Falcon). Porphyrin concentrations or saline alone (negative control) were incubated with bacteria 5 min prior to irradiation (0–30 J/cm^2) in a dark environment. Cell viability was determined by plating 20 μl of various dilutions on tryptic soy agar (TSA) plates and incubating at 37 °C overnight. Colony forming units (CFUs) were counted 18–24 h later. To elucidate the role of reactive oxygen species on bactericidal activity, reduced glutathione (10 mM) was co-administered with porphyrins 5 min preceding irradiation of 0.6 J/cm^2 and 20 J/cm^2 for MRSA and *E. coli* respectively. Bacterial killing was quantified as mentioned above.

2.5. Singlet Oxygen Production

Previous methods were used to measure steady state singlet oxygen production [27]. Briefly, porphyrins were dissolved in D_2O (10 μM) and irradiated with 405 nm LED as excitation source (60 mW). A Fluorolog® 3 Spectrofluorometer (Horiba, NJ, USA) with a liquid nitrogen-cooled indium gallium arsenide detector scanning from 1220 to 1330 nm [28] was utilized to quantify steady state singlet oxygen emission. To assess photodynamic efficiency of singlet oxygen production, spectra were corrected based on the absorbance of photosensitizer solutions (10 μM) at 405 nm using Equation 1: $\text{Em}_{\text{cor}} = \text{Em}_{\text{obs}} / (1 - 10^{-\text{Abs}})$ where Em_{cor} = corrected emission n; Em_{obs} = observed emission; Abs = absorbance at 405 nm.

2.6. Statistics

Differences between photodynamic inactivation and therapy treatment groups were determined using one-way analysis of variance (ANOVA) with Bonferroni corrections. For bacterial comparisons, the natural log of CFUs were analyzed to meet the assumptions of ANOVA. Statistical analysis was performed using Stata 12 (StataCorp LP, College Station, TX). Outcomes demonstrating $P < 0.05$ were considered statistically significant.

3. Results and Discussion

3.1. Absorption Spectra of Metalloporphyrins and Binding Affinities

For the past seventy years antibiotics have been utilized to treat a multitude of infectious diseases; however, with an absence of new antibiotics in the past thirty years, alternatives are imperative to the clinical field. One alternative is the use of photodynamic treatment encompassing a photosensitizing agent and light. The purview of this study was to assess the influence of incorporating a metal into tetra-cationic porphyrin $\text{H}_2(\text{T4})$ on photokilling against MRSA and *E. coli*.

Various metals (Cu^{2+} , Fe^{2+} , Pd^{2+} , and Zn^{2+}) were chelated by a tetracationic porphyrin ring (Fig. 1A). Normalized absorbance spectra of metalloporphyrins demonstrated a slight energy shift in the Soret peak (Fig. 1B) with Pd(T4) and Zn(T4) demonstrating the largest shift compared to the free ligand $\text{H}_2(\text{T4})$ though remaining in the violet range of the visible spectrum. Since previous studies have shown photodynamic effects are diffusion limited, it is important to demonstrate internalization or membrane-bound association of porphyrin to bacteria [29]. The extent of porphyrin binding to bacteria was approximated by assessing the residual Soret peak superimposed on the absorbance spectra of the bacterial culture. Bacterial suspensions were washed twice to ensure removal of extracellular porphyrins or those with weak affinities to bacterial membranes. Metalloporphyrin Pd(T4) binding was evident to both Gram-positive MRSA ($\text{Abs}_{418} = 0.740 \pm 0.001$) and Gram-negative *E. coli* ($\text{Abs}_{418} = 0.526 \pm 0.004$) with MRSA exhibiting 1.41 fold higher levels (Fig. 1C).

These findings support previous studies demonstrating increased uptake of meso-substituted cationic porphyrins by Gram-positive bacteria [30], primarily to the cell wall and cytoplasmic membrane [31]. Gram-positive bacteria are relatively simplistic containing a thick peptidoglycan cell wall with lipoteichoic and teichuronic acids followed by a cytoplasmic membrane. However, Gram-negative bacteria exist as a trilamellar structure with an additional outer membrane layer known as lipopolysaccharide, which is external to a thin peptidoglycan layer followed by the cytoplasmic membrane. Lipid composition of the Gram-negative outer membrane renders non-ionic and anionic photosensitizers inefficient when used in photodynamic inactivation unless co-administered with outer membrane disrupters [32]. This study affirms the binding of tetra-cationic photosensitizers to both Gram-positive and -negative bacteria.

3.2. PDI Utilizing Different Metalloporphyrins

MRSA, one of the most common causes of wound infections in the United States, continues to acquire resistance against numerous antibiotics [33,34]. This emergence strongly highlights the need for alternative treatments; thus we investigated the anti-bacterial effects of different metalloporphyrins ($\text{Cu}(\text{T4})$, $\text{Fe}(\text{T4})$, $\text{H}_2(\text{T4})$, $\text{Pd}(\text{T4})$, and $\text{Zn}(\text{T4})$) with PDI against MRSA. Bacterial cultures were pre-incubated with different concentrations of porphyrins (3, 10, or 30 μM) or sterile saline for 5 min before being irradiated for 44 s (2.5 J/cm^2) using a portable 405 nm LED. Photoinactivation with 405 nm alone has demonstrated modest anti-microbial effects against both intracellular [35] and extracellular bacteria [36–38] but only at high irradiance doses. In our studies, low irradiance doses ($\leq 2.5 \text{ J}/\text{cm}^2$) had a negligible effect (Fig. 2A) agreeing with previous studies [36,39].

Chelation of a metal by a porphyrin ring can enhance intersystem crossing [40,41], potentially leading to increased generation of reactive oxygen species (Fig. 3A). As expected, the integration of Cu^{2+} and Fe^{2+} to T4 with subsequent irradiance had a minimal effect (Fig. 2A and B) due to dissipation of energy through competing pathways [42, 43]. However, illumination with $\text{H}_2(\text{T4})$, $\text{Zn}(\text{T4})$, and $\text{Pd}(\text{T4})$ demonstrated strong anti-bacterial effects (Fig. 2). To distinguish between bactericidal and bacteriostatic activity, colony forming units (CFU) were quantified post-PDI on MRSA cultures (Fig. 2B and C). Overall, growth inhibition was more pronounced with 10 μM of photosensitizers compared to 3 μM (Fig. 2A), therefore further analysis was performed at this concentration. Dark controls with porphyrins had no significant effect on bacterial viability (Fig. 2C). Excitation with 2.5 J/cm^2 with $\text{H}_2(\text{T4})$ and $\text{Zn}(\text{T4})$ porphyrins significantly reduced MRSA CFUs by 2.4 and 2.6 \log_{10} -units respectively (Fig. 2C, $P < 0.005$), although irradiation with Pd(T4) exhibited the most pronounced bactericidal effect at 5.9 \log_{10} -units ($P < 0.005$; Fig. 2C).

3.3. Steady-State Singlet Oxygen Emission

Bactericidal effects are dependent on the production of ROS by excited porphyrins interacting with atmospheric oxygen. Although the exact mechanism is not fully detailed, there are two potential pathways. A type I mechanism consists of electron transfer-producing free radicals i.e. peroxide, superoxide, or hydroxyl radicals. Type II mechanisms involve energy transfer from the triplet excited state of the photosensitizer to molecular oxygen to create singlet oxygen [20]. Fig. 3A shows the pathway to formation of singlet oxygen (type II), which has been attributed to the photoinactivation of bacteria [39]. Upon absorption of photon, photosensitizers are promoted to excited states. By varying the metal, the electronic properties and photochemistry of each porphyrin differs, albeit subtly, in the absorption (Fig. 1B). The more drastic change is in the fate of the excited states. Introduction of a metal, specifically palladium (II), enhances spin-orbit coupling resulting in virtually complete conversion to the triplet state [27]. From the excited state, energy dissipation occurs through radiative or non-radiative pathways. The latter includes energy transfer to triplet ground state of diatomic oxygen, which transitions to highly reactive singlet oxygen as modeled in the Jablonski diagram (Fig. 3A). Photo-generated singlet oxygen can be measured by near-infrared emission [28]. As mentioned above, introducing copper or iron induces prompt quenching of the excited state; thus the absence of singlet oxygen production and negligible effects. However, emission at 1270 nm was evident amongst the remaining porphyrins yielding the following signals for $\text{H}_2(\text{T4})$ (7503), Pd(T4), (10453) and Zn(T4) (7008). Bactericidal effects at 405 nm strongly correlated to singlet oxygen formation (Fig. 2C), where Pd(T4) exhibited

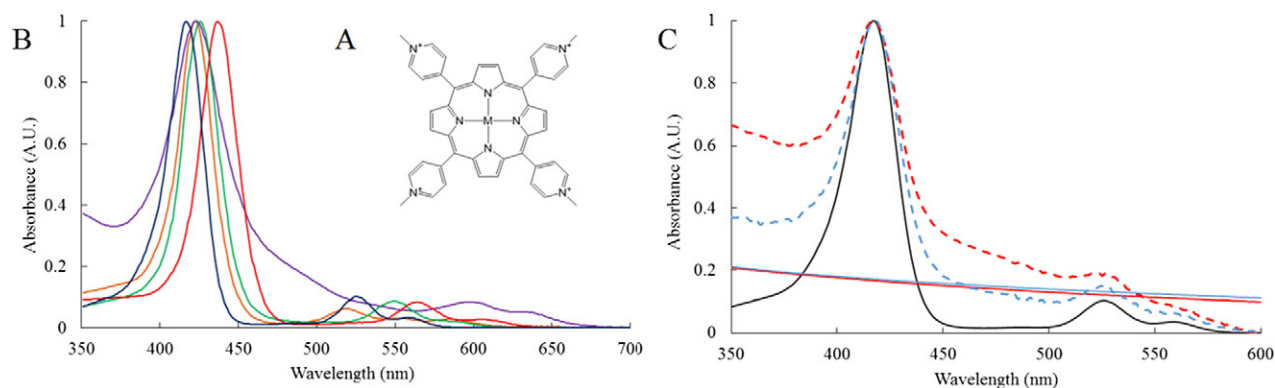


Fig. 1. Comparative spectral analysis of metalloporphyrins and their binding affinity to bacteria. (A) Structure of M(T4); where M = Cu^{2+} , Fe^{2+} , H_2 , Pd^{2+} , or Zn^{2+} . (B) Spectral differences in the normalized absorbance between various metalloporphyrins, where M = Cu^{2+} (green), Fe^{2+} (purple), H_2 (orange), Pd^{2+} (blue), or Zn^{2+} (red). To determine binding affinity of Pd(T4) to MRSA and *E. coli*, bacterial suspensions were incubated with 10 μM Pd(T4) for 5 min. (C) Normalized absorption spectra of Pd(T4) alone (solid black) was compared to MRSA (blue) and *E. coli* (red) with (dotted lines, normalized) or without (solid lines) Pd(T4). Data represent one of two independent experiments with similar findings.

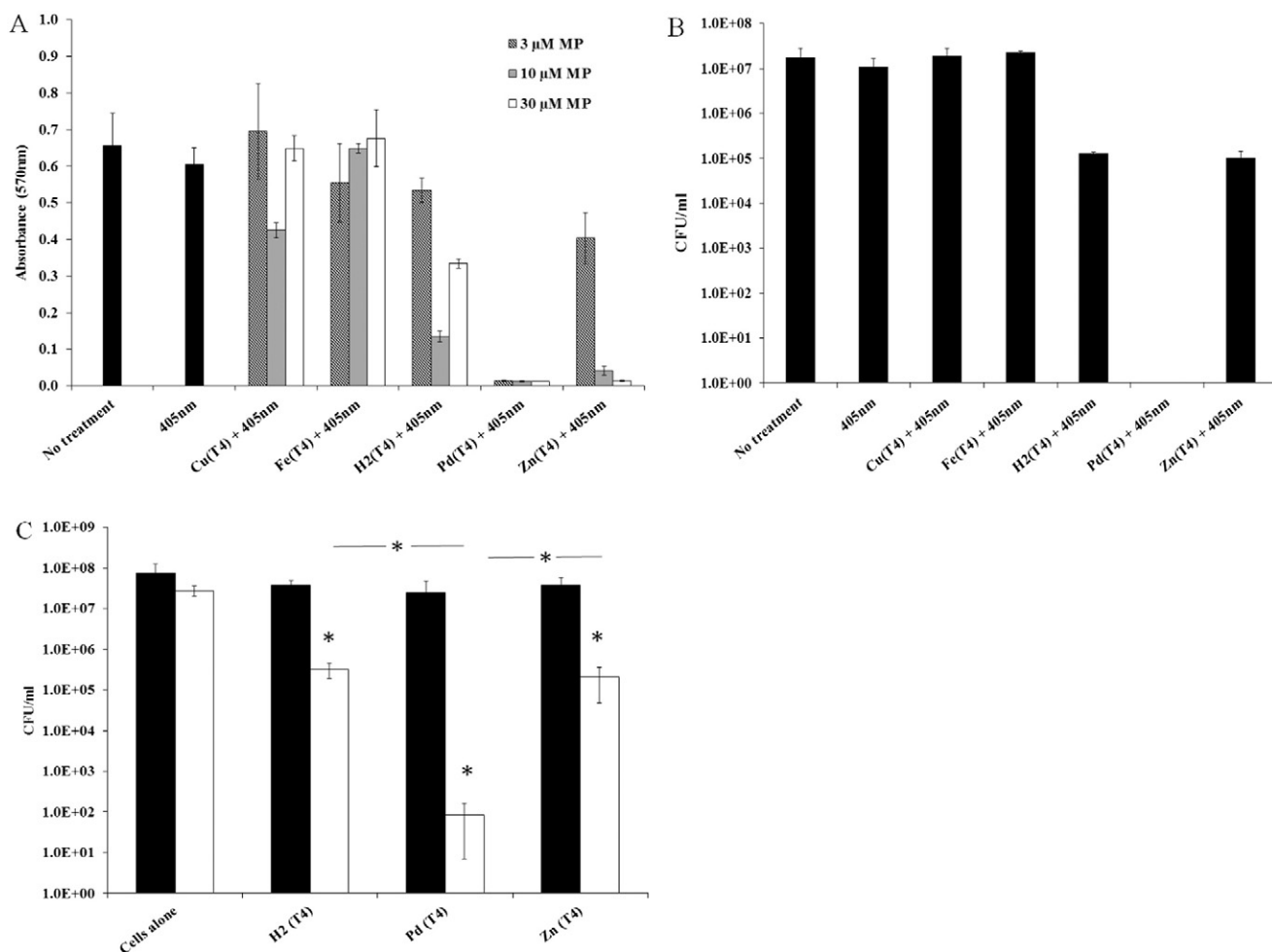


Fig. 2. Photodynamic inactivation with metalloporphyrins against MRSA. Cultures of MRSA were pre-incubated with different concentrations of various porphyrins before irradiated with 2.5 J/cm^2 of 405 nm LEDs. Bacterial viability was assessed as the mean absorbance (A) of triplicate wells from a 96-well plate \pm standard deviation after 7 h of incubation in plate shaker at 37°C or average colony counts (B) from duplicate plates \pm standard deviation 24 h post-treatment. Data are representative of one of two independent experiments both showing similar results. (C) Bacteria were incubated with $10 \mu\text{M}$ of photosensitizers with (white bars) or without (black bars) 2.5 J/cm^2 of 405 nm illumination. Values represent the means of duplicate plates from four independent experiments \pm standard deviation. * $P < 0.005$ between irradiated groups compared to no irradiation or between irradiated groups when designated by horizontal bars.

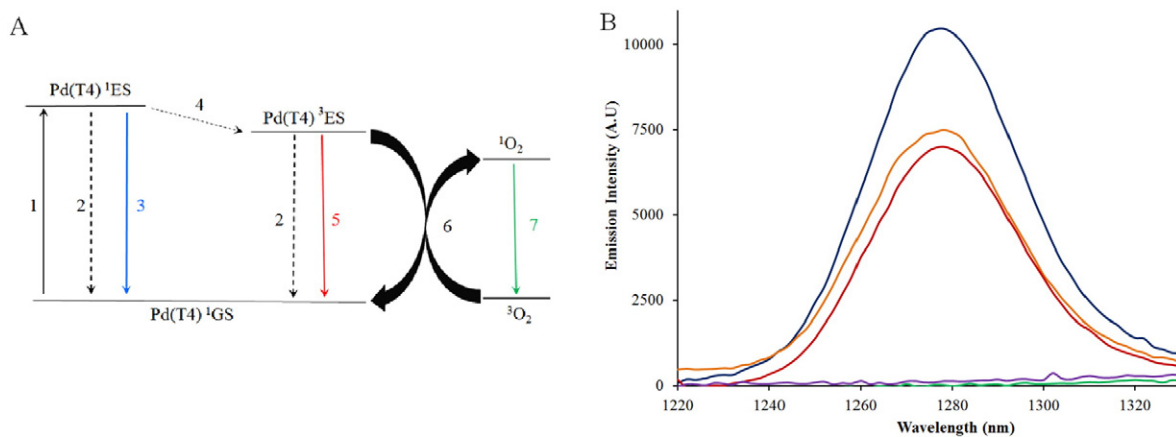


Fig. 3. Jablonski diagram and metalloporphyrin production of singlet oxygen phosphorescence subsequent to 405 nm irradiation. A modified Jablonski diagram representing singlet oxygen production via energy transfer including competing deactivation processes (A). Labeled pathways consist of: 1- absorption of photon, 2- non-radiative decay, 3- fluorescence, 4- intersystem crossing, 5- phosphorescence, 6- energy transfer, 7- singlet oxygen emission. (B) A comparative analysis of singlet oxygen emission as produced via excitation of metalloporphyrins in deuterated water (D_2O). Photosensitizers were excited with a 405 nm LED and spectral differences in singlet oxygen emission ($\sim 1270 \text{ nm}$) were quantified for various metalloporphyrins: M = Cu^{2+} (green), Fe^{2+} (purple), H_2 (orange), Pd^{2+} (blue), or Zn^{2+} (red).

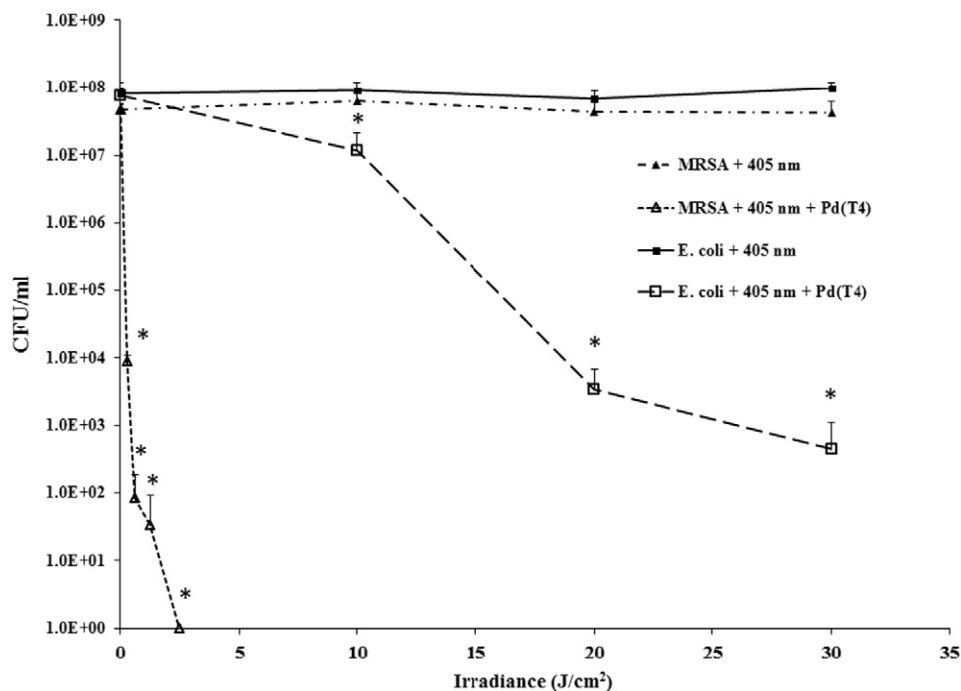


Fig. 4. Photodynamic inactivation of MRSA compared to *E. coli*. Bacterial cultures were exposed to varying energy intensities of 405 nm (MRSA: 0, 0.31, 0.63, 1.25, 2.50 J/cm² and *E. coli*: 0, 10, 20, 30 J/cm²) after a five minute pre-incubation with 10 μM Pd(T4) or saline alone CFUs were measured post-irradiation to assess viability. Results represent the mean of duplicate plates of three independent experiments ± standard deviation. Statistical differences between the means of groups with irradiation compared to no irradiation were determined using one-way ANOVA, and Bonferroni correction. **P* < 0.005.

the strongest effect. H₂(T4) and Zn(T4) porphyrins were comparable though Zn(T4) demonstrated the highest singlet oxygen yield per photon when corrected based on absorbance at 405 nm (Supplementary Fig. 1).

3.4. PDI against Gram-Positive and -Negative Bacteria

Due to variation in cell wall composition, PDI susceptibility of Gram-positive MRSA was compared to Gram-negative *E. coli*. An extra lipid

bilayer comprising the outer membrane of Gram-negative bacteria limits the susceptibility in contrast to Gram-positive [44]. Irradiation alone with 405 nm LED had minimal effect against MRSA and *E. coli* up to 30 J/cm² (Fig. 4) agreeing with previous studies [36,39]. However, in the presence of 10 μM Pd(T4) strong bactericidal effects were evident with as little as 0.3 J/cm² (5.5 s) demonstrating a reduction of 3.7 log₁₀-units (*P* < 0.005) against MRSA with complete bacterial lysis evident at 2.5 J/cm² irradiance (Fig. 4). *E. coli* displayed more resistance to PDI than MRSA but still demonstrated susceptibility (Fig. 4) exhibiting a 4.4 log₁₀

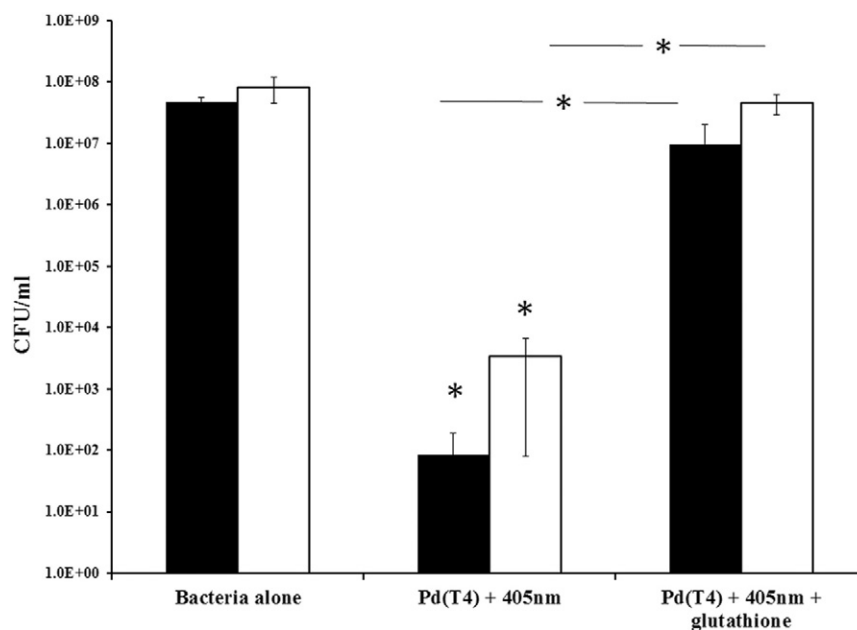


Fig. 5. Bactericidal effects of PDI are dependent on the bioactivity of reactive oxygen species. MRSA and *E. coli* were pre-incubated for 5 min with 10 μM Pd(T4) with or without reduced glutathione (10 mM) before irradiation with 0.6 J/cm² or 20 J/cm² of 405 nm LEDs respectively. Results are the mean CFUs ± standard deviation of duplicate plates of three independent experiments. Statistical differences were determined using one-way ANOVA; **P* < 0.005 comparing PDI to bacteria alone or horizontal bars comparing PDI versus PDI + glutathione.

reduction after exposure to 20 J/cm². Increased susceptibility of MRSA could be due to an array of factors. Fig. 1C supports a stronger adherence of Pd(T4) to MRSA compared to *E. coli*, suggesting closer proximity of singlet oxygen to external bacterial structures. Considering the short-lifetime (μ s) and ~ 1 μ m diffusion range [45] of singlet oxygen, adherence could have direct correlation with bactericidal activity. Photodynamic effects on *E. coli* using tetracationic porphyrins disrupt the outer membrane and cytoplasmic membranes with its corresponding enzymes like NADH and succinate dehydrogenase, and ATPase [46–49].

Bactericidal effects of PDI have been directly correlated with the production of ROS and their interactions with various molecular components like DNA, RNA, proteins, phospholipids, and cellular membranes [46,48–52]. To further confirm this method of toxicity, MRSA and *E. coli* were pre-incubated with Pd(T4) and reduced glutathione before applying a sub-lethal dose of 405 nm irradiation (0.6 and 20 J/cm² respectively). As first demonstrated in Fig. 4, a significant bactericidal effect was evident post-irradiation against both bacteria; however, addition of reduced glutathione completely abrogated bactericidal effects (Fig. 5). Reduced glutathione has been shown to deactivate singlet oxygen [53]; accordingly our results reinforce the supposition that singlet oxygen contributes the majority of photodynamic inactivation of bacteria [39].

In conclusion, photodynamic therapy continues to gain support due to its anti-microbial activity, safety, and resilience to resistance. This study compared five different photosensitizers for use in conjunction with a hand-held 405 nm LED and identified robust bactericidal effects with Pd(T4) being optimal. Treatment utilizing Pd(T4) was effective against both Gram-negative and -positive pathogens in vitro with MRSA showing increased susceptibility with photodynamic killing evident within 6 s (0.31 J/cm²). Cell death was directly correlated to the quantified singlet oxygen emission and reverted upon addition of reduced glutathione suggesting a type II mechanism. The use of a portable 405 nm LED in combination with short treatment times (seconds) supports future application as a potential industrial disinfectant and self-care treatment. Further studies utilizing Pd(T4) with 405 nm in vivo are needed to support clinical application.

Supplementary data to this article can be found online at doi:10.1016/j.jphotobiol.2016.10.016.

Acknowledgements

These studies were funded by the Student Opportunity Funds and Department of Chemical and Biological Sciences at Rockford University as well as Aqua Aerobics in Rockford, IL, USA. We would like to thank Janis Eells, Ph.D. from University of Wisconsin–Milwaukee for the donation of the WARP 405 nm LED and Jong Hyun Choi, Ph.D. from Purdue University for the use of the spectrofluorometer.

References

- Centers for Disease Control and Prevention, Antibiotic resistant threats in the United States, 2013 www.cdc.gov/drugresistance/pdf/ar-threats-2013-508.pdf.
- R.R. Roberts, B. Hota, I. Ahmad, R.D. Scott 2nd, S.D. Foster, F. Abbasi, S. Schabowski, L.M. Kampe, G.G. Ciavarella, M. Supino, J. Naples, R. Cordell, S.B. Levy, R.A. Weinstein, Hospital and societal costs of antimicrobial-resistant infections in a Chicago teaching hospital: implications for antibiotic stewardship, *Clin. Infect. Dis.* 49 (2009) 1175–1184.
- D.A. Tadesse, S. Zhao, E. Tong, S. Ayers, A. Singh, M.J. Bartholomew, P.F. McDermott, Antimicrobial drug resistance in *Escherichia coli* from humans and food animals, United States, 1950–2002, *Emerg. Infect. Dis.* 18 (2012) 741–749.
- M. Carrel, M.L. Schweizer, M.V. Sarrazin, T.C. Smith, E.N. Perencevich, Residential proximity to large numbers of swine in feeding operations is associated with increased risk of methicillin-resistant *Staphylococcus aureus* colonization at time of hospital admission in rural Iowa veterans, *Infect. Control Hosp. Epidemiol.* 35 (2014) 190–193.
- A.J. Watkinson, E.J. Murby, D.W. Kolpin, S.D. Costanzo, The occurrence of antibiotics in an urban watershed: from wastewater to drinking water, *Sci. Total Environ.* 407 (2009) 2711–2723.
- P. McGann, E. Snesrud, R. Maybank, B. Corey, A.C. Ong, R. Clifford, M. Hinkle, T. Whitman, E. Lesho, K.E. Schaecher, *Escherichia coli* Harboring *mcr-1* and *blaCTX-M* on a Novel *IncF* Plasmid: First Report of *mcr-1* in the USA *Antimicrob. Agents Chemother.* 2016.
- P.L. Graham 3rd, S.X. Lin, E.L. Larson, A U.S. population-based survey of *Staphylococcus aureus* colonization, *Ann. Intern. Med.* 144 (2006) 318–325.
- H.F. Chambers, The changing epidemiology of *Staphylococcus aureus*? *Emerg. Infect. Dis.* 7 (2001) 178–182.
- C.L. Maree, R.S. Daum, S. Boyle-Vavra, K. Matayoshi, L.G. Miller, Community-associated methicillin-resistant *Staphylococcus aureus* isolates causing healthcare-associated infections, *Emerg. Infect. Dis.* 13 (2007) 236–242.
- C. Centers for Disease, Prevention, *Staphylococcus aureus* resistant to vancomycin—United States, MMWR Morb. Mortal. Wkly Rep. 51 (2002) (2002) 565–567.
- S. Zhang, X. Sun, W. Chang, Y. Dai, X. Ma, Systematic review and meta-analysis of the epidemiology of vancomycin-intermediate and heterogeneous vancomycin-intermediate *Staphylococcus aureus* isolates, *PLoS One* 10 (2015), e0136082.
- J.L. Wardlaw, T.J. Sullivan, C.N. Lux, F.W. Austin, Photodynamic therapy against common bacteria causing wound and skin infections, *Vet J* 192 (2012) 374–377.
- J.A. dos Reis Jr., F.B. de Carvalho, R.F. Trindade, P.N. de Assis, P.F. de Almeida, A.L. Pinheiro, A new preclinical approach for treating chronic osteomyelitis induced by *Staphylococcus aureus*: in vitro and in vivo study on photodynamic antimicrobial therapy (PAmT), *Lasers Med. Sci.* 29 (2014) 789–795.
- I.T. Kato, R.A. Prates, C.P. Sabino, B.B. Fuchs, G.P. Tegos, E. Mylonakis, M.R. Hamblin, M.S. Ribeiro, Antimicrobial photodynamic inactivation inhibits *Candida albicans* virulence factors and reduces in vivo pathogenicity, *Antimicrob. Agents Chemother.* 57 (2013) 445–451.
- G.B. Kharkwal, S.K. Sharma, Y.Y. Huang, T. Dai, M.R. Hamblin, Photodynamic therapy for infections: clinical applications, *Lasers Surg. Med.* 43 (2011) 755–767.
- K. Winkler, C. Simon, M. Finke, K. Bleses, M. Birke, N. Szentmary, D. Huttenberger, T. Eppig, T. Stachon, A. Langenbacher, H.J. Foth, M. Herrmann, B. Seitz, M. Bischoff, Photodynamic inactivation of multidrug-resistant *Staphylococcus aureus* by chlorin e6 and red light ($\lambda = 670$ nm), *J. Photochem. Photobiol. B* 162 (2016) 340–347.
- L. Huang, T. Dai, M.R. Hamblin, Antimicrobial photodynamic inactivation and photodynamic therapy for infections, *Methods Mol. Biol.* 635 (2010) 155–173.
- F. Giuliani, M. Martinelli, A. Cocchi, D. Arbia, L. Fantetti, G. Roncucci, In vitro resistance selection studies of RLP068/Cl, a new Zn(II) phthalocyanine suitable for antimicrobial photodynamic therapy, *Antimicrob. Agents Chemother.* 54 (2010) 637–642.
- A. Tavares, C.M. Carvalho, M.A. Faustino, M.G. Neves, J.P. Tome, A.C. Tome, J.A. Cavaleiro, A. Cunha, N.C. Gomes, E. Alves, A. Almeida, Antimicrobial photodynamic therapy: study of bacterial recovery viability and potential development of resistance after treatment, *Mar Drugs* 8 (2010) 91–105.
- M.C. DeRosa, R.J. Crutchley, Photosensitized singlet oxygen and its applications, *Coord. Chem Rev.* 233 (2002) 351–371.
- C.S. Prasanth, S.C. Karunakaran, A.K. Paul, V. Kussovski, V. Mantareva, D. Ramaiah, L. Selvaraj, I. Angelov, L. Avramov, K. Nandakumar, N. Subhash, Antimicrobial photodynamic efficiency of novel cationic porphyrins towards periodontal gram-positive and gram-negative pathogenic bacteria, *Photochem. Photobiol.* 90 (2014) 628–640.
- M. Merchat, G. Bertolini, P. Giacomini, A. Villanueva, G. Jori, Meso-substituted cationic porphyrins as efficient photosensitizers of gram-positive and gram-negative bacteria, *J. Photochem. Photobiol. B* 32 (1996) 153–157.
- B. Marydasan, A.K. Nair, D. Ramaiah, Optimization of triplet excited state and singlet oxygen quantum yields of picolylamine-porphyrin conjugates through zinc insertion, *J. Phys. Chem. B* 117 (2013) 13515–13522.
- R.F. Pasternack, R.A. Brigandi, M.J. Abrams, A.P. Williams, E.J. Gibbs, Interactions of porphyrins and metalloporphyrins with single-stranded poly(Da), *Inorg. Chem.* 29 (1990) 4483–4486.
- R. McGuire, D.R. McMillin, Steric effects direct the binding of porphyrins to tetramolecular quadruplex DNA, *Chem. Commun.* (2009) 7393–7395.
- H.Y. Zhang, M.A. Bork, K.J. Riedy, D.R. McMillin, J.H. Choi, Understanding photophysical interactions of semiconducting carbon nanotubes with porphyrin chromophores, *J. Phys. Chem. C* 118 (2014) 11612–11619.
- M.A. Bork, C.G. Gianopoulos, H. Zhang, P.E. Fanwick, J.H. Choi, D.R. McMillin, Accessibility and external versus intercalative binding to DNA as assessed by oxygen-induced quenching of the palladium(II)-containing cationic porphyrins Pd(T4) and Pd(tD4), *Biochemistry* 53 (2014) 714–724.
- J. Baier, T. Fuss, C. Pollmann, C. Wiesmann, K. Pindl, R. Engl, D. Baumer, M. Maier, M. Landthaler, W. Baumler, Theoretical and experimental analysis of the luminescence signal of singlet oxygen for different photosensitizers, *J. Photochem. Photobiol. B* 87 (2007) 163–173.
- T. Maisch, A. Eichner, A. Spath, A. Gollmer, B. Konig, J. Regensburger, W. Baumler, Fast and effective photodynamic inactivation of multiresistant bacteria by cationic riboflavin derivatives, *PLoS One* 9 (2014), e111792.
- M.A. Pereira, M.A. Faustino, J.P. Tome, M.G. Neves, A.C. Tome, J.A. Cavaleiro, A. Cunha, A. Almeida, Influence of external bacterial structures on the efficiency of photodynamic inactivation by a cationic porphyrin, *Photochemical & photobiological sciences: Official journal of the European Photochemistry Association and the European Society for Photobiology* 13 (2014) 680–690.
- M. Merchat, J.D. Spikes, G. Bertolini, G. Jori, Studies on the mechanism of bacteria photosensitization by meso-substituted cationic porphyrins, *J. Photochem. Photobiol. B* 35 (1996) 149–157.
- M.R. Hamblin, T. Hasan, Photodynamic therapy: a new antimicrobial approach to infectious diseases? *Photochemical & photobiological sciences: Official journal of the European Photochemistry Association and the European Society for Photobiology* 3 (2004) 436–450.
- B.P. Howden, P.B. Ward, P.G.P. Charles, T.M. Korman, A. Fuller, P. du Cros, E.A. Grabsch, S.A. Roberts, J. Robson, K. Read, N. Bak, J. Hurley, P.D.R. Johnson, A.J.

- Morris, B.C. Mayall, M.L. Grayson, Treatment outcomes for serious infections caused by methicillin-resistant *Staphylococcus aureus* with reduced vancomycin susceptibility, *Clin. Infect. Dis.* 38 (2004) 521–528.
- [34] R.K. Flamm, R.E. Mendes, P.A. Hogan, J.E. Ross, D.J. Farrell, R.N. Jones, *In vitro* activity of linezolid as assessed through the 2013 LEADER surveillance program, *Diagn. Microbiol. Infect. Dis.* 81 (2015) 283–289.
- [35] C.J. Wasson, J.L. Zourelis, N.A. Aardsma, J.T. Eells, M.T. Ganger, J.M. Schober, T.A. Skwor, Inhibitory effects of 405 nm irradiation on *Chlamydia trachomatis* growth and characterization of the ensuing inflammatory response in HeLa cells, *BMC Microbiol.* 12 (2012) 176.
- [36] A. Lipovsky, Y. Nitzan, A. Gedanken, R. Lubart, Visible light-induced killing of bacteria as a function of wavelength: implication for wound healing, *Lasers Surg. Med.* 42 (2010) 467–472.
- [37] M. Maclean, S.J. MacGregor, J.G. Anderson, G. Woolsey, Inactivation of bacterial pathogens following exposure to light from a 405-nanometer light-emitting diode array, *Appl. Environ. Microbiol.* 75 (2009) 1932–1937.
- [38] A. Kumar, V. Ghate, M.J. Kim, W. Zhou, G.H. Khoo, H.G. Yuk, Kinetics of bacterial inactivation by 405 nm and 520 nm light emitting diodes and the role of endogenous coproporphyrin on bacterial susceptibility, *J. Photochem. Photobiol. B* 149 (2015) 37–44.
- [39] M. Maclean, S.J. Macgregor, J.G. Anderson, G.A. Woolsey, The role of oxygen in the visible-light inactivation of *Staphylococcus aureus*, *J. Photochem. Photobiol. B* 92 (2008) 180–184.
- [40] A. Harriman, G. Porter, P. Walters, Photooxidation of metalloporphyrins in aqueous solution, *J Chem Soc Farad T 1* (79) (1983) 1335–1350.
- [41] K. Kalyanasundaram, M. Neumannspallart, Photophysical and redox properties of water-soluble porphyrins in aqueous-media, *J Phys Chem-Us* 86 (1982) 5163–5169.
- [42] W.A. Eaton, E. Charney, Near-infrared absorption and circular dichroism spectra of ferrocyclochrom C-D→D transitions, *J Chem Phys* 51 (1969) 4502.
- [43] B.P. Hudson, J. Sou, D.J. Berger, D.R. Mcmillin, Luminescence studies of the intercalation of Cu(Tmpyp4) into DNA, *J. Am. Chem. Soc.* 114 (1992) 8997–9002.
- [44] Y. Nitzan, R. Dror, H. Ladan, Z. Malik, S. Kimel, V. Gottfried, Structure-activity relationship of porphines for photoinactivation of bacteria, *Photochem. Photobiol.* 62 (1995) 342–347.
- [45] T. Maisch, J. Baier, B. Franz, M. Maier, M. Landthaler, R.M. Szeimies, W. Baumler, The role of singlet oxygen and oxygen concentration in photodynamic inactivation of bacteria, *P Natl Acad Sci USA* 104 (2007) 7223–7228.
- [46] M.M. Awad, A. Tovmasyan, J.D. Craik, I. Batinic-Haberle, L.T. Benov, Important Cellular Targets for Antimicrobial Photodynamic Therapy *Appl Microbiol Biotechnol* 2016.
- [47] G. Valduga, B. Breda, G.M. Giacometti, G. Jori, E. Reddi, Photosensitization of wild and mutant strains of *Escherichia coli* by meso-tetra (N-methyl-4-pyridyl)porphine, *Biochem. Biophys. Res. Commun.* 256 (1999) 84–88.
- [48] B. Pudziuvyte, E. Bakiene, R. Bonnett, P.A. Shatunov, M. Magaraggia, G. Jori, Alterations of *Escherichia coli* envelope as a consequence of photosensitization with tetrakis(N-ethylpyridinium-4-yl)porphyrin tetratosylate, *Photochemical & photobiological sciences: Official journal of the European Photochemistry Association and the European Society for Photobiology* 10 (2011) 1046–1055.
- [49] D.A. Caminos, M.B. Spesia, P. Pons, E.N. Durantini, Mechanisms of *Escherichia coli* photodynamic inactivation by an amphiphilic tricationic porphyrin and 5,10,15,20-tetra(4-N,N,N-trimethylammoniumphenyl) porphyrin, *Photochemical & photobiological sciences: Official journal of the European Photochemistry Association and the European Society for Photobiology* 7 (2008) 1071–1078.
- [50] R. Dosselli, R. Millioni, L. Puricelli, P. Tessari, G. Arrigoni, C. Franchin, A. Segalla, E. Teardo, E. Reddi, Molecular targets of antimicrobial photodynamic therapy identified by a proteomic approach, *J. Proteome* 77 (2012) 329–343.
- [51] D. de Sousa Neto, A. Hawe, M. Tabak, Interaction of meso-tetrakis (4-N-methylpyridyl) porphyrin in its free base and as a Zn(II) derivative with large unilamellar phospholipid vesicles, *Eur. Biophys. J.* 42 (2013) 267–279.
- [52] M. Salmon-Divon, Y. Nitzan, Z. Malik, Mechanistic aspects of *Escherichia coli* photodynamic inactivation by cationic tetra-meso(N-methylpyridyl)porphine, *Photochemical & photobiological sciences: Official journal of the European Photochemistry Association and the European Society for Photobiology* 3 (2004) 423–429.
- [53] T.P. Devasagayam, A.R. Sundquist, P. Di Mascio, S. Kaiser, H. Sies, Activity of thiols as singlet molecular oxygen quenchers, *J. Photochem. Photobiol. B* 9 (1991) 105–116.